DOI:
10.1109/ICEAA.2019.8879106

Document Version
Peer reviewed version

Metamaterial Designs to Enhance Microwave Imaging Applications

Eleonora Razzicchia[(1)], Maria Koutsoupidou[(1),(2)], Helena Cano-Garcia[(2)], Ioannis Sotiriou[(1)], Efthymios Kallos[(2)], George Palikaras[(2)], and Panagiotis Kosmas[(1) (2)]
(1) Faculty of Natural and Mathematical Sciences, King's College London, Strand London WC2R 2LS, UK
(2) Medical Wireless Sensing Ltd, 42 New Road, London E1 2AX, UK,
e-mail: eleonora.razzicchia@kcl.ac.uk; panagiotis.kosmas@kcl.ac.uk

***Abstract*— This paper presents an innovative metasurface design for emerging microwave brain imaging applications, such as stroke detection and monitoring. We have modelled different metamaterial designs in diverse setups, and have simulated their interactions with EM waves using CST Microwave Studio®. Our results have shown an enhancement of penetration for the transmitted signals when the metamaterial film is placed in contact with skin tissue. These results suggest that our design can be a significant hardware advance towards scanners for brain imaging.**

Keywords—*microwave tomography, brain imaging, metamaterial, metasurface, split-ring resonators (SRRs), CST Microwave Studio®*

I. Introduction

Microwave imaging (MWI) for medical applications is a promising field of research, as it uses non-ionizing radiation and has the potential of leading to low-cost and portable diagnostic devices which can address specific clinical needs such as stroke detection and monitoring [1]. However, developing a MWI system for this purpose is a challenging task. An important milestone towards achieving a functional MWI system is finding a compromise between higher resolution and significant penetration depth into the tissue. Thus, a valid MWI apparatus should maximize the amount of incident power coupled into the human body and provide acceptable spatial resolution images [2].

The amount of incident power penetrating into the brain tissue must be delivered using compact antennas operating in the desired frequency range. Microwave tomography methods operate with low-power EM signals, which propagate into biological tissues in the 0.5-3.0 GHz frequency range. For stroke MWI, previous studies have demonstrated that optimal performances are achieved below 2.0 GHz [2]. This limit is due to the strong EM wave attenuation inside the human head. To couple the energy from the transmitting array into the region of interest, a dielectric medium is typically used. The use of a lossy dielectric medium reduces unwanted multipath signals [3] and broadens the frequency range of operation [4]. However, it also affects the detection of useful weak signals. Moreover, whether liquid or solid, the material is typically heavy, thick and bulky, limiting the MWI scanner's portability and ease of use.

An alternative way to achieve impedance matching and improve the transmitted power while retaining the system's small form factor is to place a metamaterial film in front of the head to act as an antireflection coating [5]. In particular, layers of split-ring resonators (SRRs) have been shown to be able to enhance the field penetration in the human tissue for several applications. In the microwave spectrum, SRRs have been already used for breast imaging [6], magnetic resonance imaging [7] and near-field imaging [8]. In addition, Mukherjee et al. have demonstrated that the resolution of microwave far field imaging could be enhanced designing a metamaterial lens based sensor. The inclusion of a lens in the sensor system provides significant benefits, such as rapid inspection and super-resolution [9]. SRR-based metamaterials have been proposed at higher frequencies for improving the impedance matching, reducing reflection, and greatly enhancing transmission [10]. In the THz spectrum, metamaterial substrates based on SRRs have been proposed to improve the antennas' gain and directivity [11][12].

In this paper, we investigate the feasibility of developing a SRR based metamaterial film to function as an impedance matching layer to enhance microwave brain imaging. Our preliminary results suggest that integrating out metamaterial design into a MWI scanner for brain stroke detection and monitoring can enhance performance by efficient impedance matching without the disadvantages of conventional dielectric materials.

II. Metamaterial Unit Cell Design

A. Metamaterial Immersed in a Dielectric Medium

A new metamaterial film comprising a copper lattice embedded between two substrates of a high permittivity dielectric has been designed. Two substrates were tested: Rogers RO3010 TM (ε'= 10.2 and tanδ = 0.0022), which is more flexible, and Rogers TMM 13i (ε'= 12.2 and tanδ = 0.0019). The two substrates are bonded with Rogers 3001 Bonding Film (ε'=2.28, tnδ = 0.003) and air is trapped between the first substrate and the bonding layer.

This metamaterial has been incorporated in a model for the human head comprising seven flat layers including skin (thickness t1 = 2.8 mm) [13], cortical bone (outer layer) (t2 = 1.8 mm), cancellous bone (t3 = 2.3 mm), cortical bone (inner layer) (t4 = 1.4 mm) [14] [15], cerebrospinal fluid (CSF) (t5 = 4.2 mm), grey (t6 = 2.5 mm) and white matter (t7 = 56.6 mm) [16]. The dielectric properties of the tissues at 1 GHz were found in [17]. The metamaterial is considered to be immersed in a dielectric medium made of 90% glycerol-water mixture, as this immersion liquid is required for our designed antennas to operate efficiently in the desired frequency range [18].

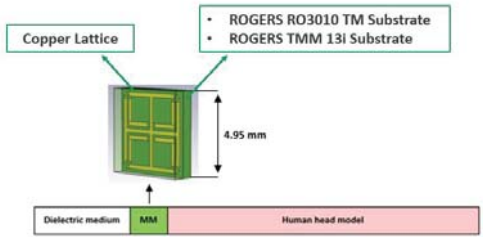

Fig. 1. Geometrical configurations of a unit cell of the metamaterial lattice and simulation setup

This setup (Fig. 1) was modelled using CST Microwave Studio® for plane wave excitation and linear polarization in the 0.5-1.5 GHz frequency range. The S-parameters were calculated in CST considering port 1 before glycerol layer (thickness tg = 9 mm, permittivity ε' = 18 and conductivity = 1.3 S/m at 1 GHz) and port 2 after white matter. The results have shown that the more flexible substrate improved transmission by about 1.50 dB at 1 GHz, whereas the use of Rogers TMM 13i led to an improvement of 1.80 dB at 1 GHz.

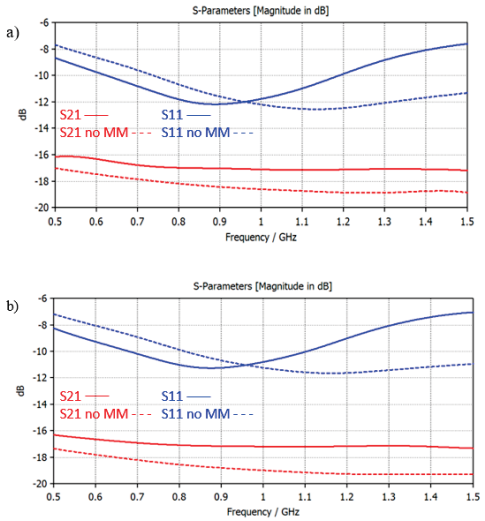

Fig. 2. Simulation results for the transmission (S21) and reflection (S11) parameters with (solid lines) and without (dashed lines) the metamaterial for Rogers RO3010 TM (a) and Rogers TMM 13i substrate (b).

B. Metamaterial placed on an Impedance-Matching Gel

The same metamaterial was then tested using a different setup, comprising an impedance-matching gel placed on the skin (thickness = 2 mm; ε' = 49.5 and conductivity 0.66 S/m) [19]. The human head model used for this setup comprises skin (thickness t1 = 6 mm), bone (t2 = 8 mm), cerebrospinal fluid (CSF) (t3 = 1 mm) and average brain (t4 = 20 mm). The reflection (S11) and transmission (S21) parameters were calculated considering port 1 before the metamaterial and port 2 after brain layer. To evaluate the effect of the metamaterial, the same setup was simulated replacing it with air.

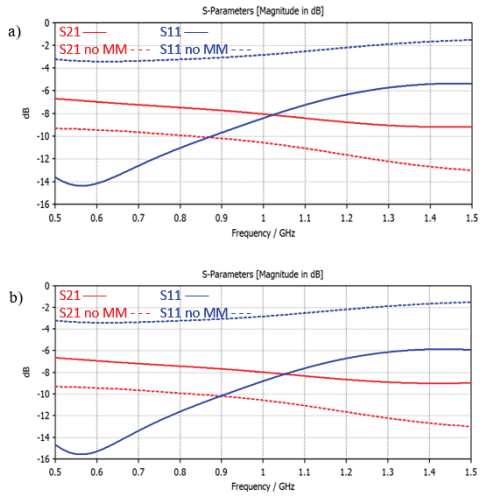

Fig. 3. Simulation results for the transmission (S21) and reflection (S11) parameters with (solid lines) and without (dashed lines) the metamaterial for Rogers RO3010 TM (a) and Rogers TMM 13i (b).

Results from these simulations are plotted in Fig.3. The MM leads to a transmission improvement of about 2.5 dB over the whole frequency range, while the electromagnetic reflection has been significantly reduced.

III. FULL METAMATERIAL STRUCTURE

A setup comprising a 15×18 unit cell metamaterial based on Rogers 3010 TM has been simulated using the antenna proposed in [18] as source of excitation. The tissue model used in this setup comprises skin (thickness t1 = 1 mm), bone (t2 = 2 mm) and brain (t3 = 7 mm). A layer of 90% glycerol-water mixture was added before the metamaterial film and the S-parameters were calculated considering the antenna as port 1 and port 2 after brain. In this case, results in Fig. 4 show an improvement in transmission of 1.30 dB at 1 GHz.

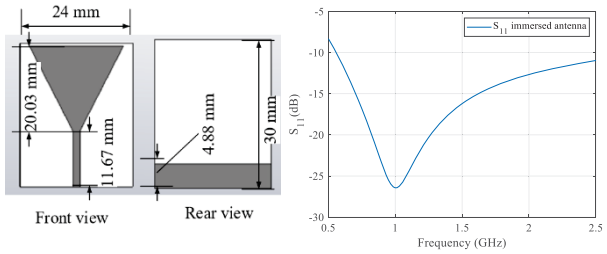

Fig. 4. Design and Reflection parameter (S11) of the proposed antenna immersed in 90% glycerol-water mixture [20].

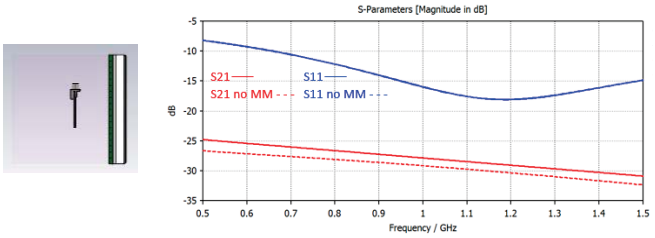

Fig. 5. Simulation setup and S-Parameters showing an improvement in transmission in the presence of the MM for the frequencies of interest.

In order to study the performance of the proposed 15×18 unit cell metamaterial layer experimentally, a new setup was modelled using CST Microwave Studio® in the 0.5-2.5 GHz frequency range. It comprises two acrylic tanks (30 cm × 30 cm × 25 cm) containing a 90% glycerol-water mixture, two antennas (one on each tank) and five tissue layers (24 cm × 21.5 cm, 1 cm thickness): skin, bone, brain, bone and skin. The different phantoms were placed in between the two tanks, supported by thin acrylic layers. The dielectric properties of the tissues at 1 GHz were found in [17].

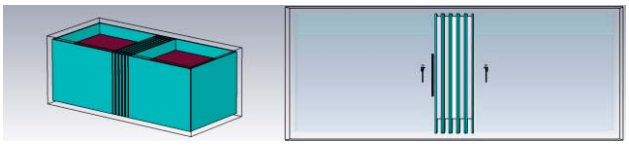

Fig. 6. Simulation setup, including two acrylic tanks filled with 90% glycerol-water mixture, five phantoms and the metamaterial layer. The metamaterial is immersed in the dielectric medium and fixed on the chamber's wall in front of Antenna 1.

First, the system was simulated without the tissue layers. The tanks and phantom's acrylic supports were filled with the lossy dielectric medium only (90% glycerol-water mixture). The antennas were placed at a distance of 13 cm and the S-

parameters were calculated with and without the metamaterial. The results have shown that the metamaterial improved transmission by about 2-3 dB over the 0.5-1.2 GHz frequency range. A second case of study includes the presence of five tissue layers between the chambers. The results have shown that the metamaterial improved transmission by about 3 dB over the 0.5-1.2 GHz frequency range.

a)

b)

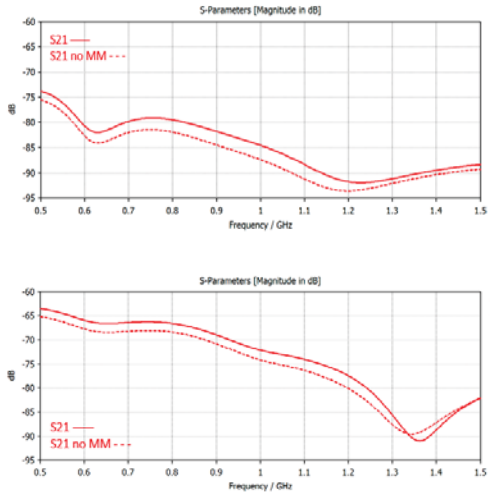

Fig. 7. Simulation results for the transmission (S21) parameter with (solid lines) and without (dashed lines) the metamaterial in presence of the dielectric medium only (a) and with phantoms (b).

The same setup was then experimentally tested. Antennas were placed at a distance of 13 cm, and the S-parameters were calculated with and without the metamaterial for the previous configurations.

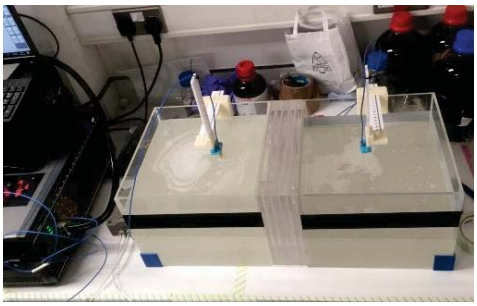

Fig. 8. Experimental setup, connected to the VNA.

Results plotted in Figs. 9, 10 show that the use of the metamaterial enhances power transmission and improves the return loss of the antenna in both the cases.

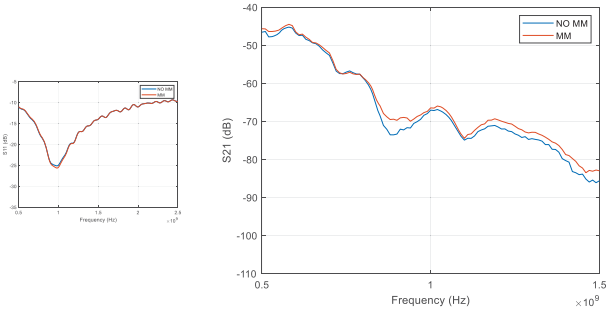

Fig. 9. Experimental results for the S11 and S21 parameters, showing an improvement in transmission when only the dielectric medium is used.

When only the dielectric medium is used without tissue-mimicking phantoms filling the liquids, the resulting improvement in transmission is around 0.9 GHz, with a maximum enhancement of 4 dB. The metamaterial leads to a transmission improvement of about 2dB from 1.2 GHz to 1.4 GHz, where the noise floor is reached.

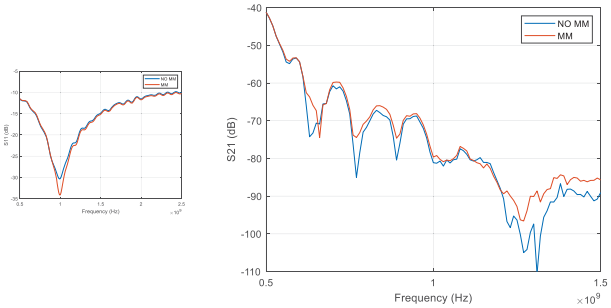

Fig. 10. Experimental results for the S11 and S21 parameters, showing and improvement in reflection and transmission in presence of phantoms.

The metamaterial has been also tested using five liquid phantoms. The phantom mixtures were obtained using different concentration of water and glycerol, in order to resemble skin, bone and brain dielectric properties. Results shows that the use of the metamaterial improved the antenna's return loss of 3.75 dB (Fig. 10). The difference in transmission is showed in Fig. 11.

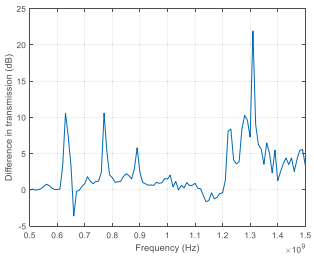

Fig. 11. Difference between the S21 parameter measured in presence of the metamaterial and the S21 parameter obtained without it, showing an overall transmission improvement, with several relevant peaks.

IV. CONCLUSIONS

We have presented an innovative metamaterial design to function as an impedance-matching layer with the potential to enhance EM wave penetration into the human head. The SRR-based metamaterial unit cell showed an improvement in transmission through a simplified layered model both when immersed in a 90% glycerol-water mixture and placed on an impedance matching gel covering the skin. After assessing the metamaterial unit cell performance, a full metamaterial structure was tested. The experimental results have shown that the metamaterial improved the antenna's return loss and the transmission whether through a lossy dielectric medium or five different phantom layers. However, creating liquid phantoms resembling the tissues dielectric properties has been a challenging task and the difference between the simulated and the experimental results might be explained taking into account eventual permittivity shifts.

In conclusion, the metamaterial design might be a significant hardware advance towards scanners for brain imaging, which can have a positive impact on MWI systems in general. However, further designs and simulation studies

must be performed, with the aim of incorporating the metamaterial design in more realistic models for the human head and the MWI systems.

ACKNOWLEDGMENT

This research was supported by the EMERALD project funded from the European Union's Horizon 2020 under the Marie Skłodowska-Curie grant agreement No. 764479. The study was also funded in part by Innovate UK grant number 103920, and in part by the Engineering and Physical Sciences Research Council grant number EP/R013918/1.

REFERENCES

[1] M. Hopfer, R. Planas, A. Hamidipour, T. Henriksson, and S. Semenov, "Electromagnetic tomography for detection, differentiation, and monitoring of brain stroke: A virtual data and human head phantom study," *IEEE Antennas Propag. Mag.*, vol. 59, no. 5, pp. 86–97, 2017.

[2] R. Scapaticci, L. Di Donato, I. Catapano, and L. Crocco, "a Feasibility Study on Microwave Imaging for Brain Stroke Monitoring," *Prog. Electromagn. Res. B*, vol. 40, no. January, pp. 305–324, 2014.

[3] P. M. Meaney, F. Shubitidze, M. W. Fanning, M. Kmiec, N. R. Epstein, and K. D. Paulsen, "Surface Wave Multipath Signals in Near-Field Microwave Imaging," *Int. J. Biomed. Imaging*, vol. 2012, no. i, pp. 1–11, 2012.

[4] C. J. Fox, P. M. Meaney, F. Shubitidze, L. Potwin, and K. D. Paulsen, "Characterization of an Implicitly Resistively-Loaded Monopole Antenna in Lossy Liquid Media," *Int. J. Antennas Propag.*, vol. 2008, no. February 2008, pp. 1–9, 2008.

[5] H. Cano-Garcia, P. Kosmas, and E. Kallos, "Demonstration of enhancing the transmission of 60 GHz waves through biological tissue using thin metamaterial antireflection coatings," *2016 10th Int. Congr. Adv. Electromagn. Mater. Microwaves Opt. METAMATERIALS 2016*, no. September, pp. 85–87, 2016.

[6] M. Koutsoupidou and I. S. Karanasiou, "Matching Medium based on Split-Ring Resonators for Microwave Breast Imaging," vol. 2015, p. 6115, 2015.

[7] M. A. Lopez, M. J. Freire, J. M. Algarin, V. C. Behr, P. M. Jakob, and R. Marqús, "Nonlinear split-ring metamaterial slabs for magnetic resonance imaging," *Appl. Phys. Lett.*, vol. 98, no. 13, pp. 1–3, 2011.

[8] S. Mukherjee, X. Shi, L. Udpa, S. Udpa, Y. Deng, and P. Chahal, "Design of a Split-Ring Resonator Sensor for Near-Field Microwave Imaging," *IEEE Sens. J.*, vol. 18, no. 17, pp. 7066–7076, 2018.

[9] S. Mukherjee, Z. Su, L. Udpa, S. Udpa, and A. Tamburrino, "Enhancement of microwave imaging using a metamaterial lens," *IEEE Sens. J.*, vol. PP, no. March, pp. 1–1, 2019.

[10] H. T. Chen, J. Zhou, J. F. O'Hara, F. Chen, A. K. Azad, and A. J. Taylor, "Antireflection coating using metamaterials and identification of its mechanism," *Phys. Rev. Lett.*, vol. 105, no. 7, pp. 1–4, 2010.

[11] M. Koutsoupidou, I. S. Karanasiou, and N. Uzunoglu, "Rectangular Patch Antenna on Split-ring Resonators Substrate for THz Brain Imaging: Modeling and Testing", 2013.

[12] M. Koutsoupidou, I. S. Karanasiou, and N. Uzunoglu, "Substrate constructed by an array of split ring resonators for a THz planar antenna," *J. Comput. Electron.*, vol. 13, no. 3, pp. 593–598, 2014.

[13] K. Chopra *et al.*, "A comprehensive examination of topographic thickness of skin in the human face," *Aesthetic Surg. J.*, vol. 35, no. 8, pp. 1007–1013, 2015.

[14] N. Lynnerup, J. G. Astrup, and B. Sejrsen, "Thickness of the human cranial diploe in relation to age, sex and general body build," *Head Face Med.*, vol. 1, no. 1, p. 13, 2005.

[15] E. M. Lillie, J. E. Urban, A. A. Weaver, A. K. Powers, and J. D. Stitzel, "Estimation of skull table thickness with clinical CT and validation with microCT," *J. Anat.*, vol. 226, no. 1, pp. 73–80, 2015.

[16] B. Fischl and A. M. Dale, "Measuring the thickness of the human cerebral cortex from magnetic resonance images.," *Proc. Natl. Acad. Sci. U. S. A.*, vol. 97, no. 20, pp. 11050–5, 2000.

[17] D. Andreuccetti, "An internet resource for the calculation of the dielectric properties of body tissues in the frequency range 10 Hz-100 GHz," Httpniremf Ifac Cnr Ittissprop, 2012.

[18] S. Ahsan, Z. Guo, Z. Miao, I. Sotiriou, M. Koutsoupidou, E. Kallos, G. Palikaras, and P Kosmas, "Design and experimental validation of a multiple-frequency microwave tomography system employing the DBIM-TwIST algorithm," *Sensors*, vol. 18, no. 10, 3491, Oct 2018.

[19] T. Sunaga et al., "Development of a Dielectric Equivalent Gel for Better Impedance Matching for Human Skin," Bioelectromagnetics, vol. 24, no. 3, pp. 214–217, 2003.

[20] S. Ahsan, M. Koutsoupidou, E. Razzicchia, I. Sotiriou, and P. Kosmas, "Advances towards the Development of a Brain Microwave Imaging Scanner," vol. 3, pp. 5–8, 2019.